Frontier-Orbital Interactions along the Intrinsic Reaction Coordinates of Ketene Dimerizations#

Shinichi YAMABE and Tsutomu MINATO*,†
Department of Chemistry, Nara University of Education, Takabatake-cho, Nara 630
†Institute for Natural Science, Nara University, 1500 Misasagi-cho, Nara 631

(Received May 13, 1993)

Ketene dimerizations to diketene and to 1,3-cyclobutanedione are studies theoretically. Their transition state (TS) structures are determined, for the first time, with correlated wavefunctions. The present calculation demonstrates that the two reactions proceed concertedly. The intrinsic reaction coordinates (IRCs) starting from the TSs are traced so as to seek the origin of the selectivity of the two reactions. At their initial stages, a one-center type charge transfer (donative orbital interaction) takes place, enhanced by polarization interactions in the charge-acceptor ketene. The back-donative orbital interactions are found to control the selectivity.

The present paper describes a theoretical study on ketene dimerizations. Ketene is known to dimerize yielding diketene in Eq. 1 and 1,3-cyclobutanedione in Eq. 2. The selectivity is that the parent ketene

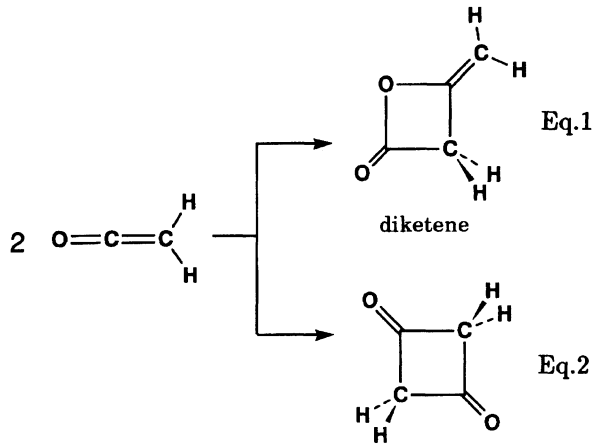

favors Eq. 1, while the substituted ketenes do Eq. 2.[1] The following 1,3-dioxetane type cycloadduct is unstable relative to diketene and 1,3-cyclobutanedione (Chart 1).[2]

Recently, ketene reactions become recognized not to follow the Woodward–Hoffmann (W–H) rule.[3] For instance, the reaction path of Eq. 2 appears to conserve the C_{2h} symmetry and indeed the orbital correlation diagram shows that the thermal C_{2h} path is symmetry-allowed. However, the transition state (TS) structure has been found to have no symmetry[4] and the C_{2h}-constraint structure has four imaginary frequencies.[4b]

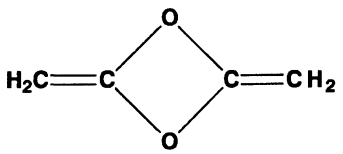

Chart 1.

#This paper is dedicated to the late Professor Hiroshi Kato.

Thus, the C_{2h} path is not the reaction route of Eq. 2. The breakdown of the W–H rule, i. e., the concept of the least-motion path is a challenging problem of the reaction mechanism.

Our preliminary communication describes that two frontier orbital (FMO) interactions, homo (the highest occupied molecular orbital of a donor)→LUMO (the lowest unoccupied molecular orbital of an acceptor) and HOMO (an acceptor)→lumo (a donor), work independently for the formation of two bonds in [2+2] cycloadditions of ketenes.[5] The results were based on the analysis of the orbital interactions involved at the early stages on the intrinsic reaction coordinates (IRCs) of three ketene reactions. However, it is still open to question how FMO interactions control the two reaction paths of ketene dimerization precisely.

It is attempted in this work to find out the origin of the selectivity of Eq. 1 and Eq. 2. We will search for IRCs starting from their TS geometries and carry out configuration analysis (CA).[6] This systematic investigation is expected to reveal quantitative orbital interactions. The findings about TS alone[4] may not be related to the quantitative orbital interactions, because the FMO interactions are based on the perturbation theory.

Method of Calculations

Ab initio calculations are performed with GAUSSIAN 92[7] installed both at CONVEX C-220 at the Information Processing Center of Nara University of Education and CONVEX C-3420 at the Computer Center of Nara University.

Ketene and TS geometries as well as those of two cycloadducts are optimized with RHF/3-21G, CISD/3-21G, and MP2/6-31G* methods. The latter two methods are needed, because TS geometries have been determined only at the Hartree–Fock level[4] and the correlated wavefunctions of TSs are not yet available. Vibrational analyses are made so as to check whether the geometries obtained here are really of TS or not.

It is examined how two reaction channels, Eqs. 1 and 2, are separated by orbital interactions at the early stage of two dimerizations. Starting from the TS geometries obtained

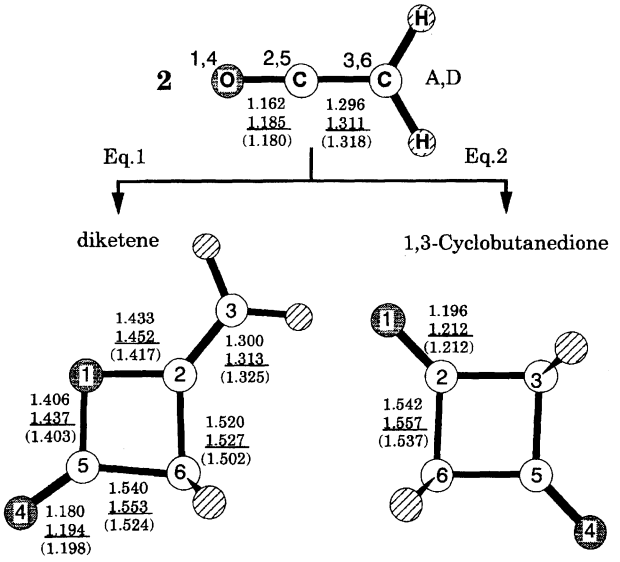

Fig. 1. Geometries of ketene and two dimerization products optimized with RHF/3-21G (plain), CISD/3-21G (underlined), and MP2/6-31G* (in parentheses) methods. The values denote bond lengths and are in Å. Left-shoulder integers attached to ketene and those in circles of cycloadducts stand for the atom numbering. "A, D" denotes an acceptor or donor ketene.

here, IRC paths[8a] are traced according to the method of Gonzalez and Schlegel.[8b] At two early stages ($s=-3.99$ and -2.99 Bohr·amu$^{1/2}$) of IRCs of Eqs. 1 and 2, CA is performed and dominant configurations are picked up.

Results of Calculation

Figure 1 shows the geometries of ketene and two dimerized products. The four-membered rings of products are planar. The correlation effect (RHF/3-21G→CISD/3-21G) on the geometries is the elongation of the convalent bonds. MP2/6-31G* calculation gives the shorter bond lengths to the four-membered rings. However, the correlation effect on the geometries is found not to be so significant.

Figure 2(a) exhibits early stages ($s=-3.99$ Bohr·amu$^{1/2}$) of the two reactions. Ketene axes are twisted with each other in the two reaction paths. The ketene A (acceptor) is bent appreciably ($\angle$CCO=166.2° in Eq. 1 and $\angle$CCO=166.8° in Eq. 2 by MP2/6-31G* method), while the ketene D (donor) retains to be linear. The ^{2}C···^{6}C distances are about 2.4 Å, indicating that this bond formation is advanced at this early stage in comparison with the ^{1}O···^{5}C or ^{3}C···^{5}C bond formation.

In the orientation of Eq. 1, a hydrogen atom of the ketene A is close to that of the ketene D. Therefore, substituted ketenes would suffer the steric repulsion in this orientation. In fact, their low reactivity for the formation of diketene is observed in contrast to the parent ketene.[1]

Figure 2 (b) shows TS structures. Each structure has a sole imaginary frequency, 637.6i or 636.1i cm^{-1}

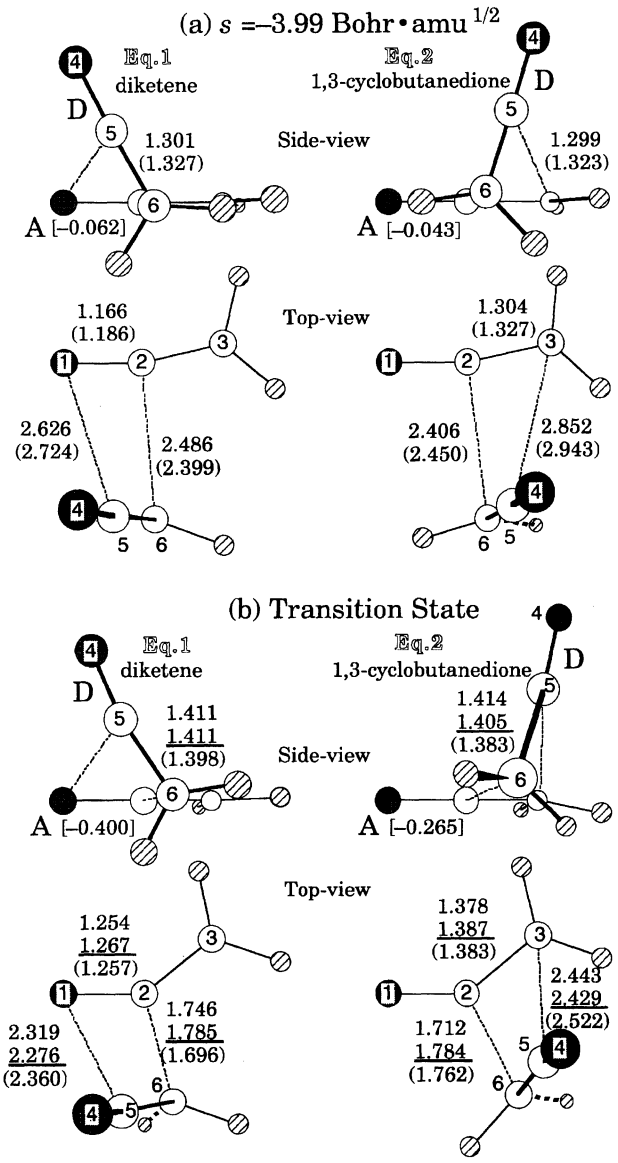

Fig. 2. Geometries of two dimerizations at (a) an early stage ($s=-3.99$) and (b) the transition state ($s=0.0$). The geometries are calculated with RHF/3-21G (plain) and MP2/6-31G* (in parentheses) method. For TS, geometric parameters with CISD/3-21G method are also shown as the underlined numbers. The bond lengths are in Å. Square-bracket numbers attached to the ketene A are net-charges (negative, charge acceptor) calculated with MP2/6-31G* method.

by CISD/3-21G method and 440.4i or 479.7i cm^{-1} by MP2/6-31G* method, as Table 1 shows. The present correlated level calculations confirm that ketene dimerizes concertedly. The side view of TS is similar to that of $s=-3.99$ Bohr·amu$^{1/2}$, which shows that the drastic geometry change does not occur during $s=-3.99$→TS. However, two points are noteworthy. One is that the ketene A becomes bent more, while the ketene D is kept to be almost linear. The other is that ^{2}C···^{6}C bonds in

Table 1. Thermochemical Properties (298.15 K)[a] and Imaginary Frequencies at Transition States for Eqs. 1 and 2

	Method	Eq. 1	Eq. 2
	RHF/3-21G	−12.6	−15.6
ΔH	CISD/3-21G	−8.6	−11.9
(kcal mol^{-1})	MP2/6-31G*	−24.5	−25.0
	Exptl.[b]	−22.0	
	RHF/3-21G	40.6	44.3
	CISD/3-21G	41.5	40.0
$\Delta H^{\ddagger}$	MP2/6-31G*	24.0	21.5
(kcal mol^{-1})	MP4/6-31G*//MP2/6-31G*	(23.6)[c]	(20.8)[c]
	Exptl.[b]	31.0	
	RHF/3-21G	−38.4	−39.7
$\Delta S^{\ddagger}$	CISD/3-21G	−38.7	−39.5
(e. u.)	MP2/6-31G*	−39.2	−39.1
	RHF/3-21G	547.7i	569.5i
$\nu^{\ddagger}$	CISD/3-21G	637.6i	636.1i
(cm^{-1})	MP2/6-31G*	440.4i	479.7i

a) The values except imaginary frequencies are evaluated as the differences between two isolated ketenes and a combined system. b) Ref. 13. c) Difference of total energy between two isolated ketenes and a transition state.

Eqs. 1 and 2 are remarkably short (1.696 Å in Eq. 1 and 1.762 Å in Eq. 2 with MP2/6-31G*) in consideration of the general TS C···C bond length, ca. 2.2 Å.[9]

The electron-charge movement along the reactions is also shown in Fig. 2(a) and (b). The net charges in square-brackets demonstrate that the ketene A is an electron acceptor. The donor (D)–acceptor (A) relation of two ketenes is one of the sources of non-W–H rule path for Eq. 2.

Table 1 summarizes the calculated thermochemical properties. MP2/6-31G* activation enthalpies ($\Delta H^{\ddagger}$ of Eq. 1>$\Delta H^{\ddagger}$ of Eq. 2) are inconsistent with experimental results. CISD/3-21G method decreases the extent of this inconsistency. Therefore, more sophisticated wavefunction would give correct $\Delta H^{\ddagger}$ values. Although Seidl and Schaefer did not discuss explicitly,[4b] single-point CI calculations on the Hartree–Fock geometry of double-zeta, double-zeta plus polarization, and triple-zeta basis sets do not remove the inconsistency. The correlation effect on the TS and IRC geometries is found to be small as Figs. 1 and 2 show. Therefore, the magnitude of orbital interactions examined in the next section is expected to be insensitive to computational methods.

Discussion of Orbital Interaction

In the previous section, the following two results emerge. The ketene A is an electron acceptor and becomes bent substantially as each reaction proceeds. The ketene D approaches the in-plane side of the ketene A with the ^{6}C–^{5}C–^{4}O axis remaining to be almost linear.

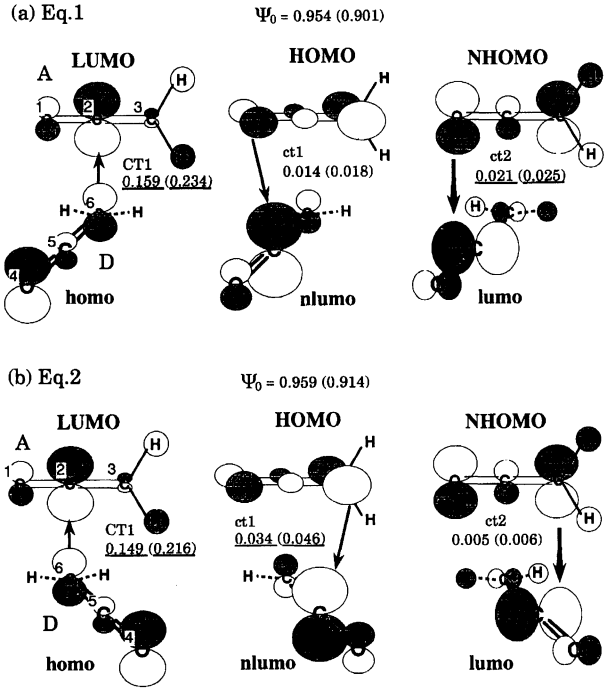

Fig. 3. Schematic presentation of dominant orbital interactions. Numbers without or with parentheses stand for the absolute values of the CA coefficients at s=−3.99 or s=−2.99 Bohr·amu$^{1/2}$ taken from Table 2.

To investigate the relation between IRC paths and orbital interaction patterns, a configuration analysis (CA) is carried out at two early stages, s=−3.99 and −2.99 Bohr·amu$^{1/2}$ of the two reactions. Table 2 displays the CA results. Figure 3 also shows important charge-transfer(CT and ct) interactions contribuitng to new bond formation. CT and ct stand for the charge transfer interaction from the ketene D to the ketene A and that from the ketene A to the ketene D, respectively. Except Ψ_0, the most important configuration is CT1 (homo→LUMO), giving rise to the advanced ^{6}C···^{2}C bond formation in both reactions. CT2 and CT3 also contribute to forming the ^{6}C···^{2}C bond. These interactions play a role as if the ketene dimerization were one-center reaction.

However, there are various back-donation configura-

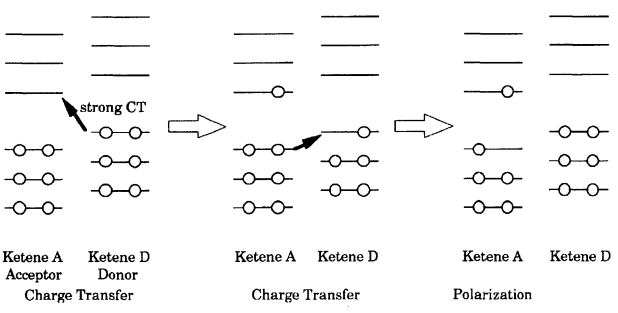

Fig. 4. Schematic presentation of polarization interaction in the ketene A.

Table 2. Coefficients of Configuration Analysis at the Early Stages of Two Dimerizations, Eqs. 1 and 2

Eq. 1 for diketene			
Configurations	Type	s (Bohr·amu$^{1/2}$)	
		−3.99	−2.99
Ψ_0		0.954	0.901
homo→LUMO (CT1)	CT	−0.159	0.234
homo→(LU+2)MO (CT2)	CT	0.035	0.034
(ho-2)mo→LUMO (CT3)	CT	−0.026	−0.033
HOMO→nlumo (ct1)	ct	(0.014)	(−0.018)
NHOMO→lumo (ct2)	ct	−0.021	−0.025
(HO-4)→LUMO	PL	0.022	0.038
(HO-2)MO→NLUMO	PL	(−0.014)	−0.026
NHOMO→LUMO	PL	−0.027	−0.048
HOMO→NLUMO	PL	(0.014)	0.029
Threshold		|0.020|	|0.025|
Eq. 2 for 1,3-cyclobutanedione			
Configurations	Type	s (Bohr·amu$^{1/2}$)	
		−3.99	−2.99
Ψ_0		0.959	0.914
homo→LUMO (CT1)	CT	0.149	0.216
homo→(LU+2)MO (CT2)	CT	−0.032	−0.031
(ho-2)mo→LUMO (CT3)	CT	−0.027	0.036
HOMO→nlumo (ct1)	ct	0.034	0.046
NHOMO→lumo (ct2)	ct	(0.005)	(0.006)
NHOMO→nlumo	ct	0.022	0.033
(HO-4)MO→LUMO	PL	0.020	0.034
NHOMO→LUMO	PL	(−0.014)	0.027
HOMO→NLUMO	PL	(0.016)	0.030
Threshold		|0.020|	|0.025|

CT and ct denote charge transfer interactions, and PL does a polarization interaction in the ketene A. HOMO, NHOMO, LUMO, and NLUMO are the highest, the next highest occupied, lowest and the next lowest unoccupied MOs, respectively, for the ketene A. The similar notations of the lower case (homo, lumo, and etc.) are used for the ketene D. (HO-4)MO is the in-plane nodeless π MO. The absolute value which is less than the threshold is shown in the parenthesis. The underlined numbers indicate the most dominant configuration in each type interaction (CT, ct, or PL). Ψ_0 means the adiabatically interacting configuration (without any electron transfer or excitation). RHF/STO-3G MOs are adopted.

tions, A→D. Among them, ct1 and ct2 appear to control the channel of either Eq. 1 of Eq. 2. In Eq. 1, ct1 (HOMO→nlumo) and ct2 (NHOMO→lumo) work cooperatively for the $^1O\cdots{}^5C$ bond formation, whereas ct1 does dominantly for the $^3C\cdots{}^5C$ bond formation in Eq. 2.

In Table 2, some polarization configurations in the ketene A(PLs) are as important as charge-transfer configurations (except Ψ_0 and CT1). These polarization interactions are caused by the succesive charge-transfer interactions, as Fig. 4 shows. That is, the succesive charge-transfer interactions are equivalent to polarization in the ketene A. The noticeable role of the polarization in the electron acceptor was pointed out previously[10] and is in line with Inagaki's postulate.[11] PLs operate to shift electronic charge from ^2C to ^1O and ^3C in the ketene A, enhancing CT1.[12] Thus, the characteristics of the ketene dimerizations is the overwhelmingly important role of CT1 assisted by PLs.

Frontier orbitals of ketene are drawn in Fig. 5. At

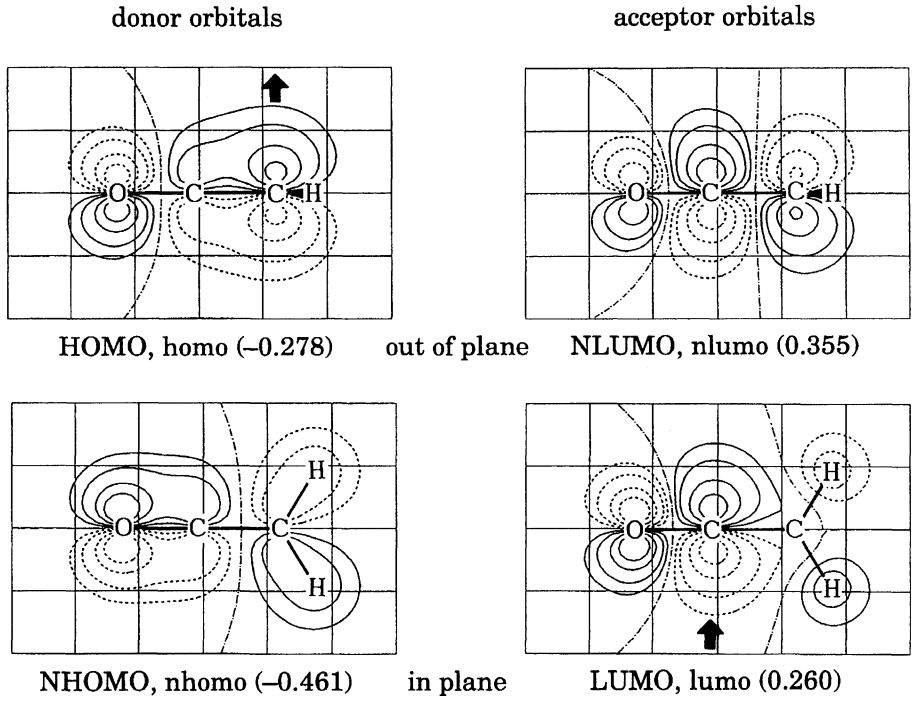

Fig. 5. Shapes of FMOs involved in orbital interactions of Table 2 and Fig. 3. Bold black arrows indicate the major reaction centers. Orbital energies in a. u. calculated by RHF/STO-3G method are also shown. Interrupted curves show nodes of orbitals.

homo (or HOMO), the methylene carbon has the largest density and is distant from the node. The distance leads the ketene D to the retention of the linearity of the ^{6}C–^{5}C–^{4}O axis (bending, unnecessary). On the contrary, LUMO must be deformed through the ^{1}O–^{2}C–^{3}C bending so as to widen the charge-acceptor region. The minor role of NLUMO in CT and ct of Table 2 is ascribed to the narrow reaction center (^{2}C) sandwiched by large different-sign lobes.

The 1,3-dioxetane product shown in Introduction is obviously unfavorable due to the absence of the $^{2}C\cdots{}^{6}C$ interaction in CT1.

Concluding Remarks

This work has dealt with two ketene dimerizations theoretically and the following results emerge. In ketene dimerizations, one of ketenes, ketene A, is a "host" molecule to accept electronic charges of a "guest" molecule, ketene D, primarily through CT1. Figure 6 shows this interaction pattern. When two ketenes approach each other, the counter-clockwise rotation of the ^{4}O–^{5}C–^{6}C axis brings about Eq. 1. On the other hand, the clockwise rotation leads to Eq. 2. Both rotations are guided by the back-donation interactions, ct1 and/or ct2. A noticeable point found here is the unexpectedly large contribution of PL interactions to enhancement of the two reactions.

In summary, ketene dimerizations occur by independent charge-transfer interactions supported by polarizations in the host ketene and are not concerned with orbital-phase properties such as a $[2\pi_a+2\pi_s]$ cycloaddition and the C_{2h} symmetry conservation.

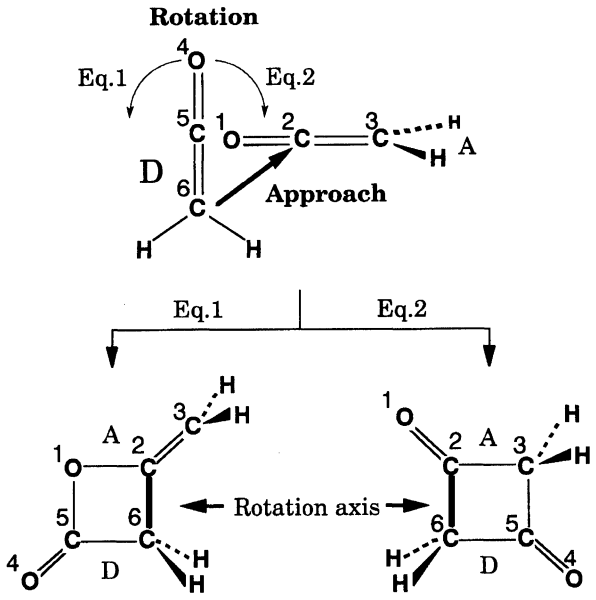

Fig. 6. A sketch of distinguishing the route Eq. 1 from Eq. 2 at the early stage of the dimerization guided by FMO interactions.

The authors thank the Information Processing Center of Nara University of Education for the allotment of the CPU time of the CONVEX C-220 computer and the Computer Center of Nara University for that of the

CONVEX C-3420 computer. The present work is supported in part by a Grant-in-Aid for Scientific Research on Priority Area "Theory of Chemical Reactions" from the Ministry of Education, Science and Culture.

References

1) R. J. Clemens, *Chem. Rev.*, **86**, 241 (1986).
2) E. T. Seidl and H. F. Schaefer, III, *J. Am. Chem. Soc.*, **112**, 1943 (1990).
3) R. B. Woodward and R. Hoffmann, "The Conservation of Orbital Symmetry," Verlag Chemie, Academic Press, New York (1970), p. 163.
4) a) X. Y. Fu, F. Decai, and D. Yanbo, *J. Mol. Struct. (Theochem)*, **167**, 349 (1988); b) E. T. Seidl and H. F. Schaefer, III, *J. Am. Chem. Soc.*, **113**, 5195 (1991); c) L. J. Schaad, I. Gutman, B. A. Hess, Jr., and J. Hu, *J. Am. Chem. Soc.*, **113**, 5200 (1991).
5) S. Yamabe, T. Minato, and Y. Osamura, *J. Chem. Soc., Chem. Commun.*, **1993**, 450.
6) H. Baba, S. Suzuki, and T. Takemura, *J. Chem. Phys.*, **50**, 2078 (1969); H. Fujimoto, S. Kato, S. Yamabe, and K. Fukui, *J. Chem. Phys.*, **60**, 572 (1974).
7) "Gaussian 92, Revision C," M. J. Frisch, G. W. Trucks, M. Head-Gordon, P. M. W. Gill, M. W. Wong, J. B. Foresman, B. G. Johnson, H. B. Schlegel, M. A. Robb, E. S. Replogle, R. Gomperts, J. L. Andres, K. Raghavachari, J. S. Binkley, C. Gonzalez, R. L. Martin, D. J. Fox, D. J. Defrees, J. Baker, J. J. P. Stewart, and J. A. Pople, Gaussian Inc., Pittsburgh, PA (1992).
8) a) K. Fukui, *J. Phys. Chem.*, **74**, 4161 (1970); b) C. Gonzalez and H. B. Schlegel, *J. Phys. Chem.*, **90**, 2154 (1989).
9) K. N. Houk, Y.-T. Lin, and F. K. Brown, *J. Am. Chem. Soc.*, **108**, 554 (1986).
10) S. Nagase, T. Fueno, S. Yamabe, and K. Kitaura, *Theor. Chim. Acta (Berlin)*, **49**, 309 (1978).
11) S. Inagaki, H. Fujimoto, and K. Fukui, *J. Am. Chem. Soc.*, **97**, 6108 (1975).
12) S. Yamabe and T. Minato, *J. Org. Chem.*, **26**, 2972 (1983).
13) J. S. Chickos, E. D. Sherwood, Jr., and K. Jug, *J. Org. Chem.*, **43**, 1146 (1978).